SYNTHESIS, CHARACTERIZATION AND BIOCOMPATIBILITY STUDY OF HYDROXYAPATITE-MAGNESIUM OXIDE NANOCOMPOSITES FOR *IN VIVO* AND *IN VITRO* ORTHOPAEDIC APPLICATIONS*

Cho Lwin Lwin Khine[1], San Nwe Zin[2], Aye Win Oo[3], Ni Ni Sein[4]

Abstract

Hydroxyapatite (HAp) materials are very popular for bone restoration. The application of pure hydroxyapatite are restricted to non load-bearing implants due to the poor mechanical properties of hydroxyapatite. To improve the mechanical properties of hydroxyapatite prepared from cow bone, incorporation of magnesium oxide was conducted in this research. Hydroxyapatite-Magnesium oxide nanocomposites (5 % and 10 %) were prepared at 1000 °C and 1100 °C. Crystal structures of all HAp-MgO nanocomposites and HAp were indexed as hexagonal. FT IR spectral data revealed the characteristic peaks of both HAp and MgO in the prepared nanocomposites. HAp-10 % MgO nanocomposites calcined at 1100 °C was found to have the highest hardness value of 53 N. HAp and HAp-MgO nanocomposites prepared at 1000 °C and 1100 °C showed no cytotoxic effect according to brine shrimp lethality bioassay. *In vitro* protein adsorption test and *in vitro* hemolysis test indicated that the prepared HAp and HAp-MgO nanocomposites were biocompatible. Orthopaedic application of HAp and HAp-MgO nanocomposites were conducted by *in vivo* study using Wistar rats. X-ray diagnosis showed that HAp-MgO nanocomposites were suitable for treatment of bone defect. *In vitro* study for repairing the non-living broken bones by HAp-MgO nanocomposites was also conducted using chicken femur bone and it was found that the composites could be used as bioglue.

Keywords: cow bone, hydroxyapatite, HAp-MgO nanocomposites, protein adsorption, hemolysis, orthopaedic application

[1]. Dr, Demonstrator, Department of Chemistry, University of Yangon
[2]. Dr, Associate Professor, Department of Chemistry, Bago University
[3]. Dr, Head of Research Officer, Laboratory Animal Services Division, Department of Medical Research (Lower Myanmar)
[4]. Dr, Professor (Retd.), Department of Chemistry, University of Yangon
* Best Paper Award Winning Paper in Chemistry, (2018)

Introduction

Hydroxyapatite is a significant biomaterial in the health care industry. Its chemical and mineral phases are analogous to those of natural bone and hence, its usage in the field of dentistry and orthopedics has been explored (Hornez *et al.*, 2007). Properties like osteoconductivity and osteoinductivity enhance bone regeneration and make hydroxyapatite an important material in tissue engineering (Burg *et al*., 2000), and its biocompatibility leads to its use as bioactive coating over implants (Ye and Wang, 2007). However, the brittleness and poor performance of mechanical stability of pure hydroxyapatite limit its use for the regeneration of non-load-bearing bone defects and tissue engineering applications (Rajkumar *et al*., 2010). Composite biomaterials like metal and polymer matrix are used to improve the mechanical compatibility of nano hydroxyapatite. Generally, composite biomaterials are prepared by using biocompatible/biodegradable and synthetic/natural polymers (Wang *et al.,* 2007). Inorganic minerals such as hydroxyapatite, bioactive glasses metal oxides and carbon nanotube are incorporated into polymer matrixes to impart bioactivity (Dhanalakshmi *et al.*, 2012). The addition of nanosized particles is desirable to develop composite with a good mechanical strength similar to the natural bone which contains mineral crystals at the nanometer scale and embedded in the collagen matrix (Joseph and Tanner, 2005).

The natural-biological origin hydroxyapatite has several important advantages: worldwide availability in almost unlimited supply, very low cost of raw materials, utilization of very simple and inexpensive apparatus, rapid, uncomplicated and very efficient transformation from raw materials into hydroxyapatite. Therefore, it seems to be an alternative for numerous products based on synthetic hydroxyapatite.

MgO is one of the most successful candidates of reinforcement oxides. The mechanical and biodegradable properties of MgO added composites and alloys are especially attractive for bone and teeth implant applications due to its excellent biocompatibility, high degradability, low weight and density similar to natural bones. MgO included HAp are widely used as bone graft materials due to faster recovery of host material (bone) by gradually releasing Mg ions from implanted materials. The MgO inclusion into the pure HAp

powder is strongly expected to affect the grain growth in HAp and improves the mechanical properties of HAp significantly (Gautam *et al*., 2016).

This research is aimed to synthesize biocompatible HAp-MgO nanocomposites from waste cow bone for orthopaedic application.

Materials and Methods

Sample Collection

Waste cow bone samples were collected from Mingalar Taung Nyunt retail market in Yangon Region.

Synthesis of HAp-MgO Nanocomposites

HAp powder was prepared by using readily affordable biowaste cow bone employing simple unit operations and acid-alkali processes (Cho Lwin Lwin Khine *et al*., 2017). For HAp-MgO, firstly MgO (5 g) was dispersed in 20 mL of distilled water with the help of a magnetic stirrer for 1 h. The hydroxyapatite suspension was also prepared using the ratio of 1:1 for powder (100 g) and water (100 mL) by means of magnetic stirring for 1 h to get homogeneity of the dispersion. To prepare HAp-5 % MgO nanocomposite, the prepared suspension was poured into the HAp solution and then was thoroughly mixed using stirrer at 80-90 °C for 1 h. The suspension was cooled to room temperature for 12 h and kept undisturbed for aging. It was then filtered and the residues were washed 2 to 3 times with distilled water. Then, it was transferred into porcelain basin and placed in an oven at 120 °C for 4 h. The resulting products were annealed at 1000 °C and 1100 °C for 4 h.

Characterization Techniques

Phase analysis and purity of prepared HAp-MgO nanocomposites were investigated by X-ray analysis. X-ray diffraction patterns of the samples were recorded on X-ray diffractometer (Rigaku, Tokyo, Japan), using CuK_{α} radiatio (λ= 1.54 Å) at 40 kV and 40 mA. The diffraction angle ranged from 10^{o} to 70^{o} of 2θ. The crystallite size was calculated by Scherrer method. Fourier transform infrared (FT IR) spectra of the samples was recorded on a FT IR

spectrometer (FT IR-8400 SHIMADZU, Japan). FT IR analysis was in a range of wavenumber from 4000 to 440 cm^{-1}.

pH and Hardness of the Prepared HAp-MgO Nanocomposites

pH values of HAp-MgO nanocomposites were determined by a pH meter (Jenway 4330, England) and the hardness of prepared HAp-MgO nanocomposites were determined by hardness tester (PHAMA Test, PTB 302).

Cytotoxicity Test

The brine shrimp (*Artemia salina*, fairy shrimp or sea monkeys) was used in this study for cytotoxicity bioassay of the prepared HAp-MgO nanocomposites (Ali *et al*., 2013). The toxicity of samples were tested at various concentrations *viz.* 1,10, 100 and 1000 µg/mL in seawater. Ten nauplii were used in each test. Three replications were used for each concentration. A parallel series of tests with the standard potassium dichromate solution and caffeine were conducted. After 24 h, the number of dead brine shrimps was counted and 50 % lethality dose (LD_{50}) was calculated (Sahgal *et al*., 2010).

Biocompatibility Tests
Protein adsorption test

Protein adsorption test was conducted according to Mishra (2013) with some modifications. Adsorbate used was Bovine Serum Albumin (BSA) from Sigma. Firstly,1 mL each of HAp-MgO nanocomposites samples with concentrations of 10 mg/mL was added to 1mL of aqueous solution of BSA (1200 µ g/mL) in respective test tubes. The mixtures were then shaken and incubated at the physiological temperature (37 ^{o}C) for 24 h. After 24 h of incubation, the samples were centrifuged at 3000 rpm for 10 min. The supernatants were removed and the residual protein concentration was determined using Biuret assay at 550 nm (Holme and Peck, 1998). Sample solution (1 mL) and 4 mL of Biuret reagent were thoroughly mixed and kept at room temperature for 30 min. After that, the absorbance value was measured at 550 nm. Hence, by difference the residual protein amount from the total protein amount, the protein adsorbed (µ g) was determined.

Hemolysis test

Hemolysis test was conducted according to Mishra (2013) with some modifications. Blood was collected from central ear artery of two white rabbits by needle. The rabbits were provided by Laboratory Animal Service, Department of Medical Research, Yangon. Trisodium citrate as anticoagulant was immediately added. The noncoagulant blood was diluted with normal saline (10 mL of normal saline per 8 mL of blood) and stored at 4 °C till use. Following this, the test specimens (10 mg each) were placed in test tubes with phosphate buffered saline (1 mL each) and agitated and incubated for 24 h at 37 °C before being exposed to blood. After that, 0.5 mL of blood was added to each test tube and the volume made up to 10 mL with saline. Hydrochloric acid was used as positive control and phosphate buffer saline (PBS) solution was used as negative control. The samples and controls were placed in contact with blood for 1 h in incubator at 37 °C. After centrifugation at 4000 rpm for 10 min, the absorbance of the supernatant was measured at 545 nm. The percentage of hemolysis was determined by the following formula.

$$\text{Percent hemolysis} = \frac{\left(A_{\text{sample}} - A_{\text{negative control}}\right)}{\left(A_{\text{positive control}} - A_{\text{negative control}}\right)} \times 100$$

***In Vivo* Test for Orthopaedic Application of HAp-MgO Nanocomposites**

HAp-MgO nanocomposites were conducted for orthopaedic application employing Wistar rats (male with 250-300 g body weight). The animals were obtained from Laboratory Animal Service Division, Department of Medical Research, Yangon. All of the rats were kept in standard rat cages. The animals were facilitated with standard environmental condition of photoperiod (12:12 h dark: light cycle) and temperature (24 °C). They were provided with standard laboratory pellets and water was given *ad libitum*. Animals were divided into two individual groups in this experiment as follows;

Group I, after surgery procedure, left side of skull defect was not filled any materials. Group I, after surgery procedure, right side of skull defect was filled with HAp. Group II, after surgery procedure, left side of skull defect was filled with HAp-5 % MgO nanocomposite at 1100 ºC. Group II, after

surgery procedure, right side of skull defect was filled with HAp-10 % MgO nanocomposite at 1100 ºC.

Wistar rats were injected with Ketamine hydrochloride (50 mg/kg) before the surgery. The dorsal area of each rats skull was shaved before the surgery, and the surgical field was prepared with septidine solution. A 3 cm midline scalp incision was made, and underlying musculature and periosteum were elevated, exposing the parietal bones. Identical 0.3 cm diameter (left side and right side) round bony defect was then created in the parietal bone using stainless steel hand drill carefully. Care was then taken to avoid injury to the dura or midsagittal sinus. The nanocomposite powder was taken in a watch glass and distilled water added drop wise till the powder got fully wet and got paste. The paste was molded in the skull bone cavity before suturing. Defects were gently packed with HAp paste for right side of test (I) animal and left side was left unfilled (control) and HAp-10 % MgO nanocomposite at 1100 ºC paste for right side of test (II) animal and HAp-5 % MgO nanocomposite at 1100 ºC paste for left side of test (II) animal. External examination of the skull bone defects was conducted after 15 days and 30 days surgery by taking photos of the skull bone. Test animals of groups (I) and (II) were post-tested by X-ray radiography. The Wistar rats were observed (a) immediately on operation day (b) 15 days after surgery and (c) 30 days after surgery at Crown Veterinary Resources, Yankin Township, Yangon. Skull bone lesion samples were used for histological examination in Pathology Research Division, Department of Medical Research (Lower Myanmar).

In Vitro Test for Orthopaedic Application (as Bone Glue) of HAp-MgO Nanocomposites

Chicken femur bones were also used *in vitro* bone glue experiment. With a manual bone saw shaft, femur bones of some of the chicken were horizontally and completely cut and some were almost completely. Bone glue made of HAp-MgO nanocomposites and polyethylene glycol (1:1) were then applied to stick the broken dried chicken femur bones and kept for 24 h.

Results and Discussion

Characterization of HAp-MgO Nanocomposites

XRD analysis

HAp-MgO nanocomposites was prepared using HAp calcined at 900 ^{o}C and MgO obtained by heating $Mg(OH)_2$ at 600 ^{o}C. Two different weight percentages of 5 % and 10 % magnesium oxide were added into HAp sample in this study.

HAp calcined at 900 ^{o}C showed well-resolved XRD pattern (Figure 1) which could be easily indexed on the basis of hexagonal crystal system with equal length of a and b axes (9.4009 Å) and shorter length of c axis (6.8757 Å). When the prepared magnesium oxide sample obtained at 600 ^{o}C was subjected to XRD analysis three well-defined diffraction peaks were observed at Miller indices of (111), (220) and (200) (Figure 2). After incorporation of magnesium oxide to HAp, the XRD patterns of HAp-MgO nanocomposites showed two new peaks corresponding to magnesium oxide peaks at (200) and (220) in addition to HAp peaks (Figure 3).

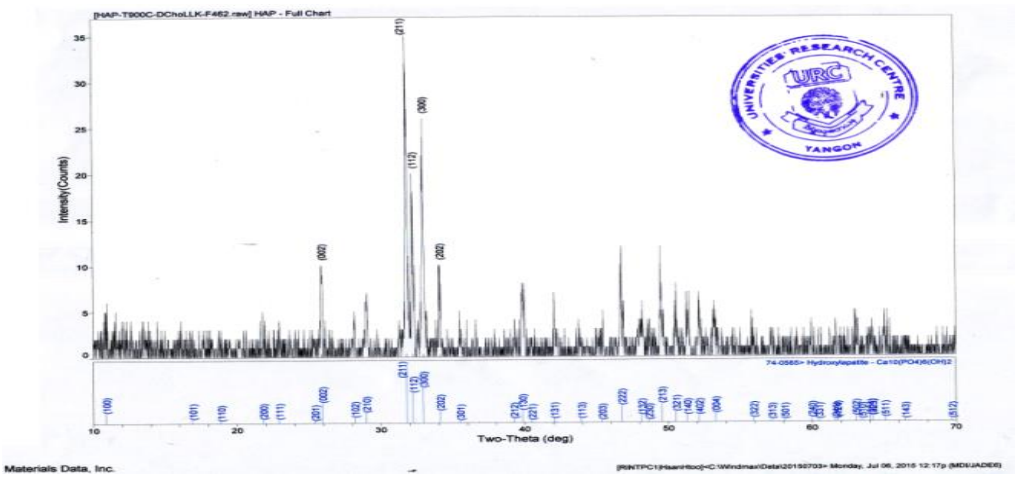

Figure 1: X-ray diffractogram of hydroxyapatite

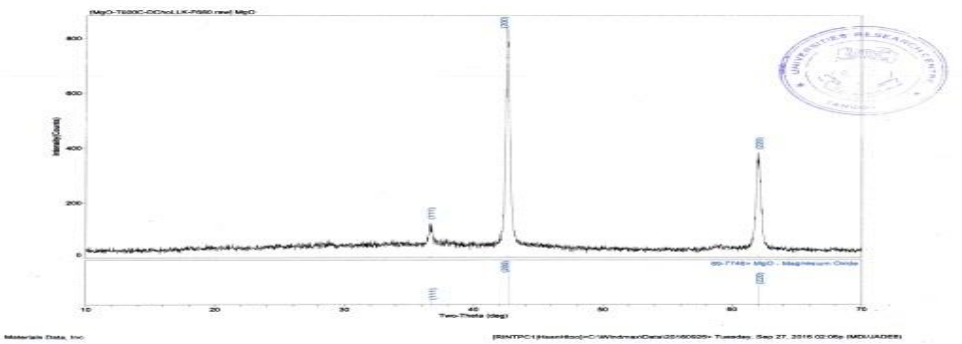

Figure 2: X-ray diffractogram of magnesium oxide obtained at 600 °C

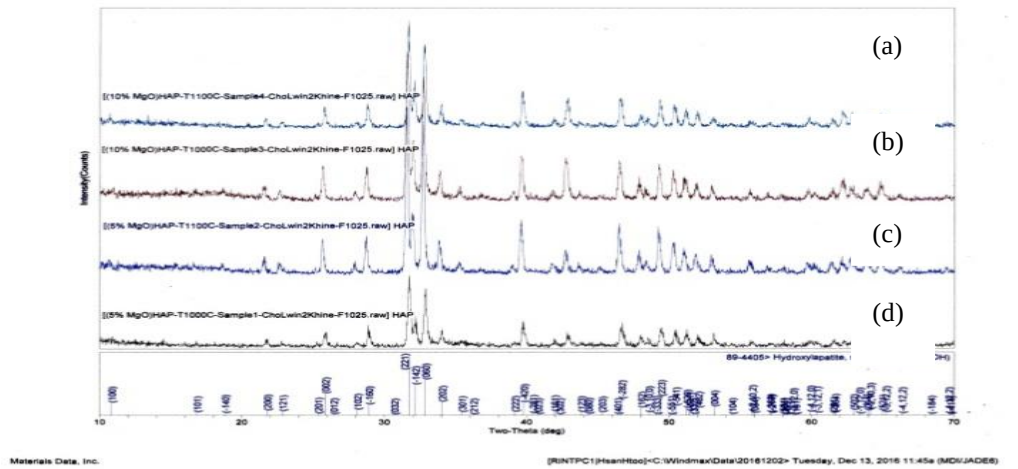

Figure 3: X-ray diffractograms of HAp-MgO nanocomposites
(a) HAp-10 % MgO (1100 ^{o}C) (b) HAp-10 % MgO (1000 ^{o}C)
(c) HAp-5 % MgO (1100 ^{o}C) (d) HAp-5 % MgO (1000 ^{o}C)

With increase in temperature the crystallite size of HAp-MgO nanocomposites were found to increase. However, the results were reversed as the amount of magnesium oxide was increased (Table 1). For HAp, the crystallite size was 69.92 nm. Crystallite sizes of HAp-MgO nanocomposites were 32.17 nm and 37.87 nm for HAp-5 % MgO nanocomposites calcined at 1000 °C and 1100 °C, respectively. For HAp-10 % MgO nanocomposites the crystallite sizes were 31.46 nm and 36.70 nm, respectively for calcination temperature of 1000 °C and 1100 °C.

Table 1: Average Crystallite Sizes, Lattice Constant and Crystal Structure of HAp-MgO Nanocomposites

No.	Sample	Average crystallite size (nm)	Lattice constant (Å)		Crystal structure
			a=b	c	
1	HAp	69.92	9.4009	6.8757	Hexagonal
2	HAp-5 % MgO nanocomposite (1000 ^{o}C)	32.17	9.5469	6.8434	Hexagonal
3	HAp-5 % MgO nanocomposite (1100 ^{o}C)	37.87	9.5998	6.9544	Hexagonal
4	HAp-10 % MgO nanocomposite (1000 ^{o}C)	31.46	9.5650	6.7985	Hexagonal
5	HAp-10 % MgO nanocomposite (1100 ^{o}C)	36.70	9.5295	6.8878	Hexagonal

Crystal structures of HAp and all of the HAp-MgO nanocomposites were hexagonal. The lattice constants of HAp-MgO nanocomposites noticeably changed from those of HAp indicating the formation of composites. Among the HAp-MgO nanocomposites, the lattice constants changed slightly with change in temperature and amount of magnesium oxide.

FT IR analysis

FT IR spectral data revealed the assignment of the vibration bands of HAp-MgO nanocomposites together with the characteristic peaks of both HAp and MgO (Table 2). The characteristic peaks of HAp in nanocomposites were observed between 700-500 cm^{-1} due to P-O bending vibration and between 1200-900 cm^{-1} due to P-O stretching vibration (Karthikeyan *et al.*, 2016). Similarly, the characteristic peaks of MgO in HAp-MgO nanocomposites were observed at 474 cm^{-1} (Nakamoto, 1970).

pH and Hardness of HAp-MgO Nanocomposites

HAp calcined at 900 ^{o}C was found to have pH value of 9.6 (Table 3). Addition of MgO nanoparticles in HAp caused slight decrease in pH values. All of the HAp-MgO nanocomposites samples and HAp sample were found to have alkaline in nature.

Hardness of HAp prepared from cow bone was found to be 12 N. Hardness increased as the amount of the addition of MgO increased in the range of 19 N to 53 N. With same composition of MgO, hardness increased as the temperature was increased. HAp- 10 % MgO at 1100 ^{o}C was found to have the highest hardness value of 53 N.

Table 2: FT IR Spectral Data of HAp, MgO and HAp-MgO Nanocomposites

No.	Wavenumber (cm^{-1})						Reported values (cm^{-1})	Remark
			HAp-MgO Nanocomposites					
	HAp (900°C)	MgO (600°C)	5 % (1000°C)	5 % (1100°C)	10 % (1000°C)	10 % (1100°C)		
1.	3697		3570	3570	3510	3568	3500-3100*	Vibration of O-H
2.	3443	3440	3427	3419	3479	3443	3444**	O-H stretching vibration of physically absorbed water molecules
3.	1456		1460	1462	1460	1462	1629-1400*	Carbonate group
4.	1413		1413	1413	1413	1413		
5.	1089		1091	1089	1091	1091	1200-900*	P-O stretching of phosphate
6.	1047		1047	1047	1047	1047		
7.	962		960	960	960	960		
8.	877						871*	Carbonate group
9.		653					650-450**	Mg-O deformation vibration
10.	632		632	632	632	634	700-500*	P-O bending of phosphate
11.	601		601	601	601	601		
12.	570		569	570	569	569		
13.		474	472	474	474	474	650-450**	Mg-O deformation vibration

***** Nakamoto, 1970 ** Karthikeyan *et al.*, 2016

Table 3: pH and Hardness of HAp and HAp-MgO Nanocomposites

No.	Samples	pH	Hardness(N)
1	HAp	9.0	12
2	HAp-5 % MgO Nanocomposite (1000 °C)	9.3	19
3	HAp-5 % MgO Nanocomposite (1100 °C)	9.5	31
4	HAp-10 % MgO Nanocomposite (1000 °C)	9.5	42
5	HAp-10 % MgO Nanocomposite (1100 °C)	9.4	53

Cytotoxicity

Brine shrimp cytotoxicity bioassay was used for the cytotoxicity test of HAp-MgO nanocomposites. Brine shrimp was used for this assay (Tawhawa, 2006). This was expressed in terms of mean ± SEM (standard error mean) and LD_{50} (50 % Lethality Dose). The data are described in Table 4. According to Meyer's toxicity index, the sample with LD_{50}<1000 μ g/mL are considered as toxic, while the sample with LD_{50} > 1000 μ g/mL are considered as non-toxic (Meyer *et al*., 1982). The prepared HAp-MgO nanocomposites were found to be noncytotoxic in the brine shrimp bioassay so they can be used as biomaterial.

Table 4: Cytotoxicity of HAp and HAp-MgO Nanocomposites

Samples	Percentage of dead brine shrimp (Mean ± SEM) in various concentrations (μg/mL)				LD_{50} (μg / mL)
	1	10	100	1000	
HAp	0 ± 0	0 ± 0	3.3 ± 1.90	6.7 ± 11.54	> 1000
A 1	0 ± 0	0 ± 0	3.3 ± 1.90	3.3 ± 1.90	> 1000
A 2	0 ± 0	0 ± 0	3.3 ± 1.90	3.3 ± 1.90	> 1000
B 1	0 ± 0	0 ± 0	6.7 ± 11.54	6.7 ± 11.54	> 1000
B 2	0 ± 0	0 ± 0	3.3 ± 1.90	6.7 ± 11.54	> 1000
*Caffeine	0 ± 0	0 ± 0	9.58 ± 0.92	12.73 ± 4.10	> 1000
*$K_2Cr_2O_7$	48.63±19.19	73.13 ±4.08	74.67 ±11.8	100 ± 0	1.5

* = used as cytotoxic standard

A 1 = HAp-5 % MgO nanocomposite (1000 °C)

A 2 = HAp-5 % MgO nanocomposite (1100 °C)

B 1 = HAp-10 % MgO nanocomposite (1000 °C)

B 2 = HAp-10 % MgO nanocomposite (1100 °C)

Protein adsorption

Cellular response on the implant after implantation depends on the initial amount of serum proteins that get adsorb to the implant.

Among the HAp-MgO nanocomposites, protein adsorption capacity increased and found to be in the range of 72.07 μg/10 mg to 90.09 μg/10 mg (Table 5). It may be due to the decrease of the crystallite size and hence, increase of surface area of the nanocomposites. In other words protein adsorption increases with increase in surface area of the samples where the crystal size is small (Feng *et al*., 2002).

Table 5: Protein Adsorption Capacities of HAp Prepared from Cow Bone (900^{o}C) and HAp-MgO Nanocomposites with Different Concentrations of MgO at Different Temperatures*

No.	Samples	Residual protein (μg/10 mg)	Protein adsorption (μg/10 mg)	Mean (μg/10 mg)
1.	HAp	1145.95	54.05	
		1167.57	32.43	54.05 ± 21.63
		1124.32	75.68	
2.	HAp-5 % MgO	1124.32	75.68	
	nanocomposite (1000 ^{o}C)	1145.95	54.05	75. 68 ± 21.63
		1102.70	97.30	
3.	HAp-5 % MgO	1102.70	97.30	
	nanocomposite (1100 ^{o}C)	1145.95	54.05	72. 07 ± 22.50
		1135.13	64.87	
4.	HAp-10 % MgO	1091.89	108.11	
	nanocomposite (1000 ^{o}C)	1113.51	86.49	90.09 ± 16.52
		1124.32	75.67	
5.	HAp-10 % MgO	1102.70	97.30	
	nanocomposite (1100 ^{o}C)	1135.13	64.87	82. 88 ± 16.53
		1113.51	86.49	

*Initial protein in 1 mL sample = 1200 μg/10 mg

Hemolysis

The prepared composites were tested for hemolytic activity and the results obtained were quite satisfactory (Table 6). The results obtained clearly indicated that, with incorporation of MgO content, the extent of hemolysis slightly increased. The observed results may be attributed to the reason that, with the incorporation of MgO in the composite, the surface composition favorably changes, which increased the hemolytic property of the material. Among the composites the hemolysis percentages did not change appreciably. If hemolysis percentage is below 2 % the material is considered non-hemolytic, between 2 % and 5 % slightly hemolytic, and above 5 % it is considered hemolytic (Laranjeiraa *et al.,* 2016). All the samples were found to have hemolysis percentages less than 5 %. Thus, these samples exhibit good biocompatibility and may be suitable biomaterials for clinical implant purposes.

Table 6: Hemolysis Percentage of HAp Prepared from Cow Bone (900 ^{o}C) and HAp-MgO Nanocomposites with Different Concentrations of MgO at Different Temperatures*

No.	Samples	Absorbance of test sample	Hemolysis (%)	Mean (%)
1.	HAp	0.096	1.61	
		0.099	1.91	1.71 ±0.17
		0.096	1.61	
2.	HAp-5 % MgO nanocomposite (1000 ^{o}C)	0.099	1.91	
		0.101	2.11	1.94 ±0.15
		0.098	1.81	
3.	HAp-5 % MgO nanocomposite (1100 ^{o}C)	0.102	2.21	
		0.099	1.91	1.98 ±0.21
		0.098	1.81	
4.	HAp-10 % MgO nanocomposite (1000 ^{o}C)	0.097	1.71	
		0.101	2.11	1.94 ±0.21
		0.100	2.00	
5.	HAp-10 % MgO nanocomposite (1100 ^{o}C)	0.099	1.91	
		0.103	2.31	2.11 ±0.20
		0.101	2.11	

*Absorbance of negative control = 0.080
Absorbance of positive control = 1.077

In Vivo Orthopaedic Application of the Prepared HAp-MgO Nanocomposites

HAp, HAp-5 % MgO (1100 ^{o}C) and HAp-10 % MgO (1100 ^{o}C) nanocomposites were separately applied as bone cement on skull bones of Wistar rats (Figure 4). The progress of these operation skull bone were recorded by the photos at specified time interval and the recorded photographs are shown in Figure 5. After 15 days, the hairs of the Wistar rats were started to grow and after 30 days it was found to be normal.

The Wistar rats were radiographed on the operation day, after 15 days and 30 days of operation (Figure 6). Bone gap were found to be 0.28 cm for control, 0.30 cm each for HAp and HAp-10 % MgO nanocomposite (1100 ^{o}C) and 0.32 cm for HAp-5 % MgO nanocomposite (1100 ^{o}C) (Table 7). After 15 days of operation, bone gap was found to decrease to 0.10 cm in control and 0.08 cm in Wistar rat filled with HAp (Table 8). This means that tiny bony defects were still observed in these rats. However, complete bone healing was observed for Wistar rats filled with nanocomposites. The composites bridged the defects and new bonds were formed. After 30 days of operation the defects were completely filled in all Wistar rats whether unfilled or filled with HAp and HAp-MgO nanocomposites (Table 9). It was found that application of HAp-MgO nanocomposites for bone defect enhanced bone healing effect compared to control and HAp only. Due to histological findings (Tables 10 and 11), HAp-10 % MgO nanocomposite at 1100 °C group is the best in the good scoring within 30 days after application.

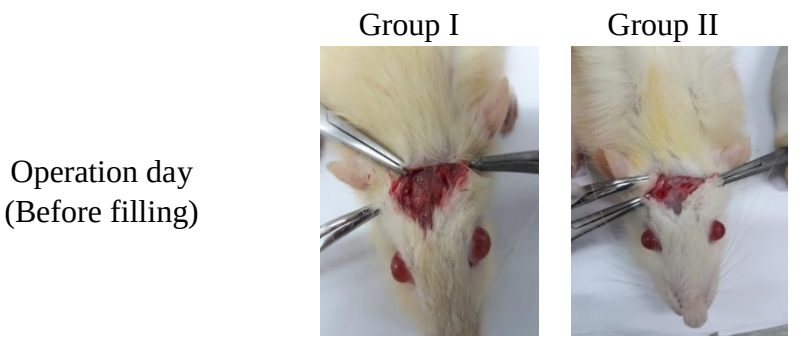

(a)

Filling
(After surgery)

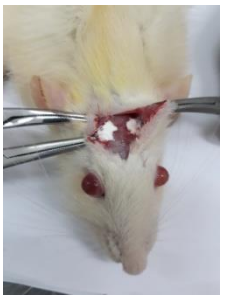

(b)

Suturing and dressing
(After filling)

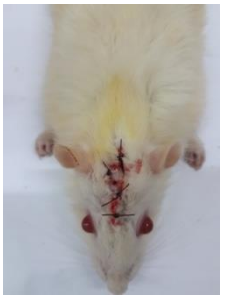

(c)

Figure 4 : Surgical procedure (a) skin incision in the dorsal portion of skull bone with surgical knife (b) filling the skull bone cavity (c) closing with suturing cat gut continuously and dressing with septidine solution

Group I

(a)

(b)

(c)

Group II

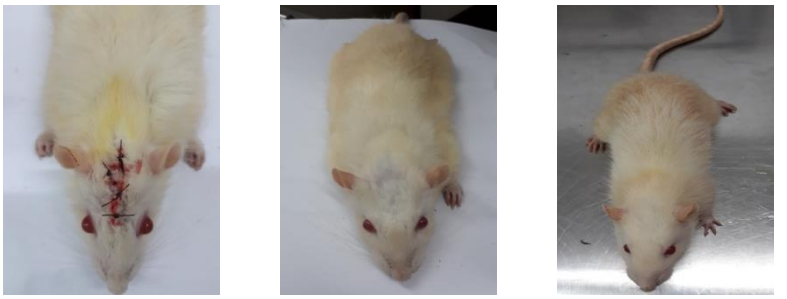

(a) (b) **(c)**

Figure 5: External feature of the skull bone defect healing progressiveness of Wistar rats
(a) Operation day
(b) 15 days after surgery
(c) 30 days after surgery

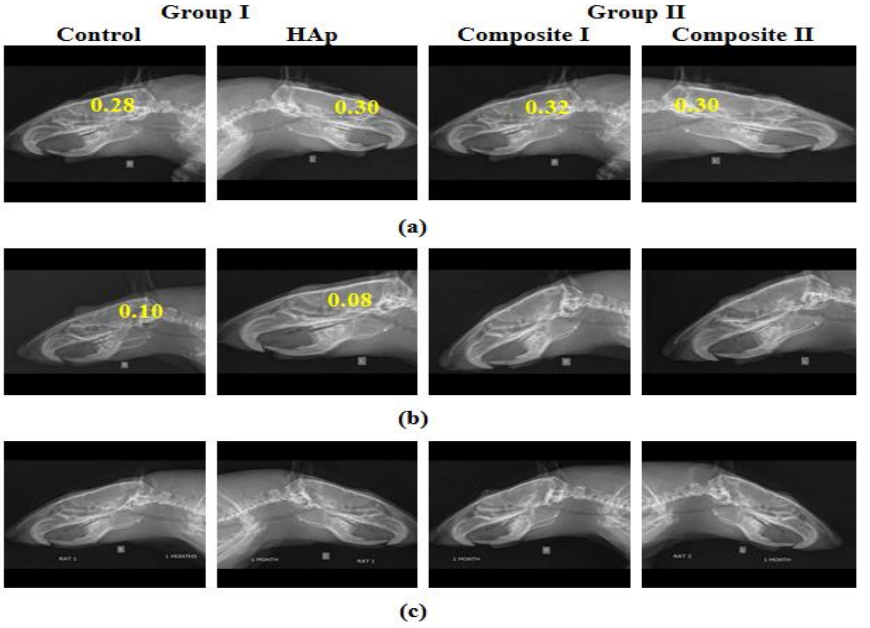

Figure 6 : Progressiveness of skull bone defect healing in X-ray view of Wistar rats
(a) Operation day
(b) 15 days after surgery
(c) 30 days after surgery

Composite I = HAp-5 % MgO nanocomposite (1100 ^{o}C)
Composite II = HAp-10 % MgO nanocomposite (1100 ^{o}C)

Table 7: Examination of Skull Bone Defect by X-ray Radiography (Operation day)

Samples	Condition	X-ray diagnosis	X-ray picture
Control	Unfilled defect	Incomplete filling (Bone cavity gap = 0.28 cm)	
HAp	HAp (900 ºC)	Incomplete filling (Bone cavity gap = 0.30 cm)	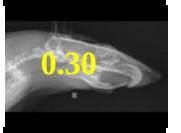
Composite I	HAp-5 % MgO nanocomposite (1100 ºC)	Incomplete filling (Bone cavity gap = 0.32 cm)	
Composite II	HAp-10 % MgO nanocomposite (1100 ºC)	Incomplete filling (Bone cavity gap = 0.30 cm)	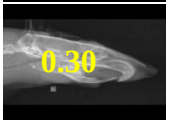

Table 8: Examination of Skull Bone Defect by X-ray Radiography (15 days after Surgery)

Samples	Condition	X-ray diagnosis	X-ray picture
Control	Unfilled defect	A tiny hole bone defect remaining (Bone cavity gap = 0.10 cm)	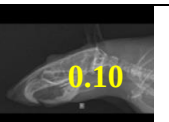
HAp	HAp (900 ºC)	Remaining very little pointed bony defect to become completely (Bone cavity gap = 0.08 cm)	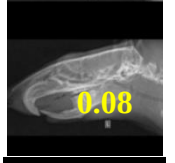
Composite I	HAp-5 %MgO nanocomposite (1100 ºC)	Complete bone healing bridge the defect (No bone cavity gap)	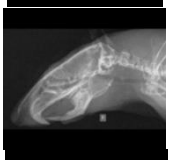
Composite II	HAp-10 %MgO nanocomposite (1100 ºC)	Complete bone healing bridge the defect (No bone cavity gap)	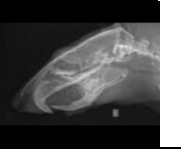

Table 9: Examination of Skull Bone Defect by X-ray Radiography (30 days after Surgery)

Samples	Condition	X-ray diagnosis	X-ray picture
Control	Unfilled defect	Complete bone healing bridge the defect (No bone cavity gap)	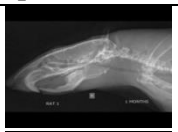
HAp	HAp (900 ºC)	Complete bone healing bridge the defect (No bone cavity gap)	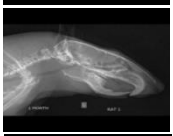
Composite I	HAp-5 % MgO nanocomposite (1100 ºC)	Complete bone healingbridge the defect (No bone cavity gap)	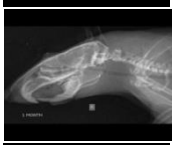
Composite II	HAp-10 % MgO nanocomposite (1100 ºC)	Complete bone healing bridge the defect (No bone cavity gap)	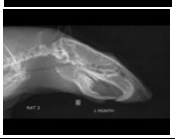

Histopathological report of 15 days and 30 days skull bone healing of the Wistar rats using prepared HAp and HAp-MgO nanocomposites

Histology features of bony healing (15 days after operation) are shown in Table 10.

Table 10: Histological Report of Bone Healing (15 Days after Operation)

No.	Slide Image	Histology Description	Bony Healing Results
1.	Control 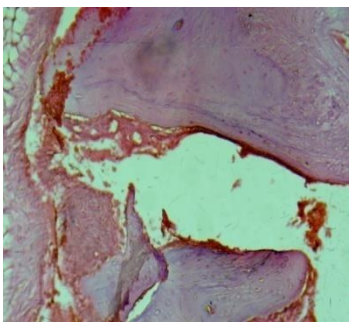	Histology of fracture skull bone revealed that connective tissue was occupied especially fibroblast and admixed with net work of delicate bone trabeculae lined with osteoblast and formed from inner surface of wall of skull bone. Blood clot remnants were observed.	Score - 0 Non-union of skull bone

2.	HAp 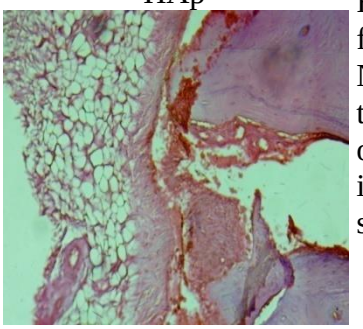	Fracture site was filled with fibroblast and blood clots. Net work of delicate bone trabeculae lined with osteoblast and formed from inner surface of wall of skull bone.	Score- 1 Incomplete cartilage union
3.	Composite I 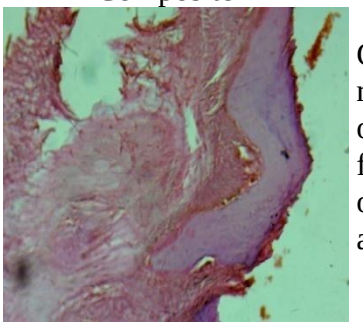	Coagulum (blood clot) was reduced in size and observed woven bone formation composed of few osteoblast and increased amount of chondrocytes.	Score- 2 Complete with cartilage union
4.	Composite II 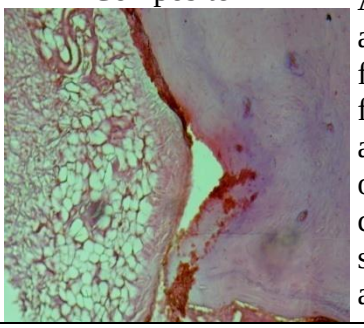	A few coagulum was found and mixed with few fibroblast. Woven formation was noted and accompanied with increased osteoblast and chondrocytes. A fracture site was replaced by few amount of trabecular bone.	Score -3 Predorminantly cartilage with some trabecular bone

Histology features of bony healing (30 days after operation) are shown in Table 11.

Table 11: Histological Report of Bone Healing (30 Days after Operation)

No.	Slide Image	Histology Description	Bony Healing Results
1.	Control 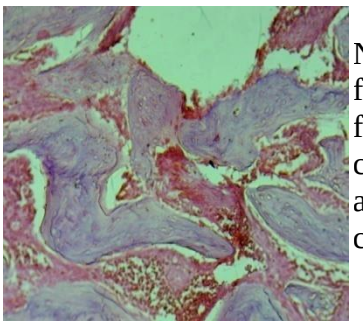	New trabecular bone formation was started from fracture site and composed of osteoblast and increased amount of chondrocytes.	Score - 3 Predorminantly cartilage with some trabecular bone
2.	HAp 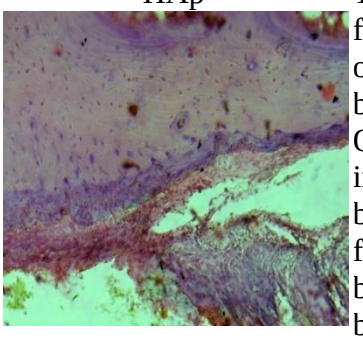	Trabecular bone formation was well organized and absence of blood clots and fibroblast. Osteoblast was seen in inner layer of fracture bone. Chrondrocytes were filled in some trabecular bone areas. Incomplete bony union with intermediate ossification was observed.	Score-4 Equal amounts of cartilage and trabecular bone
3.	Composite I 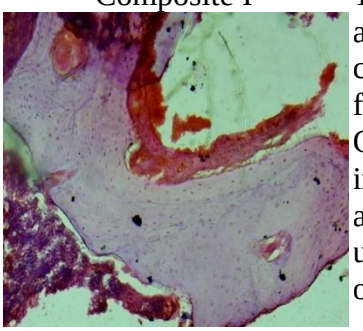	There was increased amount of osteocytes in centre area of bony fracture site. Chrondrocytes were filled in some trabecular bone areas. Incomplete bony union with late ossification was observed.	Score-5 Predorminantly trabecular bone with some cartilage

4.	Composite II		
	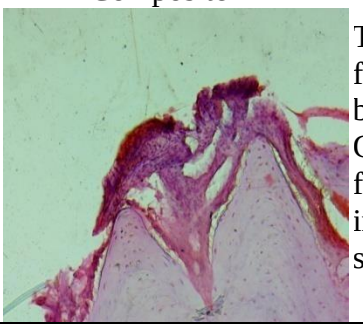	There was complete new formation of trabecular bone in fracture site. Complete union of fracture area was observed in entire bony fracture site.	Score-6 Complete union of fractured bone

***In Vitro* Orthopaedic Application of the Prepared HAp-MgO Nanocomposites (Bone Glue)**

Since HAp-MgO nanocomposites has low adhesive property of non-living bone, addition of polyethylene glycol to HAp-MgO nanocomposites with ratio of 1:1 (w/w) was prepared and the paste was used as bone glue for the broken non-living chicken femur bone in this study. After application of the prepared bone glue on the intentionally broken femur bone, it was observed that HAp-MgO nanocomposites and polyethylene glycol particles adhered to the bone.

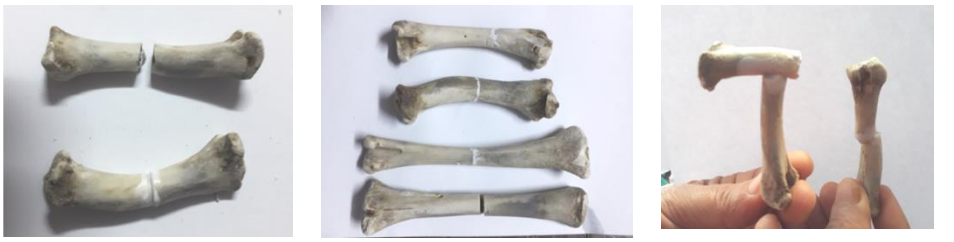

(a) (b) (c)

Figure 7: HAp-10 % MgO nanocomposite (1100 °C) as bone glue for broken chicken femur bone
(a) completely cut bone (broken straight across)
(b) almost completely cut bone
(c) connection of two pieces of bone

Conclusion

HAp-MgO nanocomposites were successfully prepared using natural HAp from waste cow femur bone in order to enhance the bioactivity of the HAp, to improve the mechanical properties and to increase its potential use as scaffold for bone tissue engineering application in this research. Increase in hardness was observed after incorporation with magnesium oxide. Brine shrimp cytotoxic assay showed that the composites were noncytotoxic. Protein adsorption test and hemolysis test revealed that HAp-MgO nanocomposites were found to be biocompatible with living tissue. HAp-MgO nanocomposites promoted the bone healing activity of HAp. *In vitro* study of HAp-MgO nanocomposites as bioglue showed a good adherence between the two non-living broken bones. Thus, the composites can be used as bioglue in museums for repairing the broken bones. These results indicate that the prepared HAp-MgO nanocomposites has demonstrated better osteoconductive and osteopromotive abilities with faster proliferation of new bone tissue formation than HAp.

Acknowledgements

The authors would like to express their profound gratitude to the Department of Higher Education, Ministry of Education, Myanmar for provision of opportunity to do this research. Professor Dr Hnin Hnin Aye (Head of the Chemistry Department) for her support and staff members from Department of Medical Research (Lower Myanmar) for their cooperation.

References

Ali, N., Allen, U., Shaha, S. W. A., Shaha, I., Junaid, M., Ahmed, G., Ali, W. and Ghias, M. (2013). "Acute Toxicity, Brine Shrimp Cytotoxicity, Anthelmintic and Relaxant of Fruits of *Rubus fruiticosis* Agg". *BMC Complement. Alter. Med.*, vol. 13, pp. 138-143

Burg, K. J. L., Porter, S. and Kellam, J. F. (2000). "Biomaterial Developments in Bone Tissue Engineering". *Biomaterials*, vol. 21, pp. 2347-2359

Cho Lwin Lwin Khine, San Nwe Zin and Ni Ni Sein. (2017). **"**Effect of Calcination on Morphological, Structural and Thermal Properties of Hydroxyapatite (HAp) Prepared from Cow Bone". *J. Myan. Acad. Tech*., vol. 17(1), pp. 68-81

Dhanalakshmi, C. P., Vijayalakshmi L. and Narayanan. V. (2012). "Synthesis and Preliminary Characterization of Polyethylene Glycol (PEG)/ Hydroxyapatite (HAp) Nanocomposite for Biomedical Applications". *International Journal of Physical Sciences*, vol. 7(13), pp. 2093-2101

Feng, B., Chen, J. and Zhang, X. (2002). "Interaction of Calcium and Phosphate in Apatite Coating on Titanium with Serum Albumin". *Biomaterials*, vol. 23, pp. 2499-2507

Gautam, C. R., Kumar, S., Biradar, S., Jose, S., and Mishra, V. K. (2016). "Synthesis and Enhanced Mechanical Properties of MgO Substituted Hydroxyapatite: A Bone Substitute Material". *Royal Society of Chemistry Adv.*, vol. 6(72), pp. 67565-67574

Holme, J. D. and Peck, H. (1998). *Analytical Biochemistry*. London : 3rd Ed., Longman, pp. 390-391

Hornez, J. C., Chai, F., Monchau, F., Blanchemain, N., Descamps, N. and Hildebrand, H. F. (2007). "Biological and Physico-chemical Assessment of Hydroxyapatite (HA) with Different Porosity". *Biomol. Eng*., vol. 24, pp. 505-509

Joseph, R. and Tanner, K. E. (2005). "Effect of Morphological Features and Surface Area of Hydroxyapatite on the Fatigue Behavior of Hydroxyapatite-Polyethylene Composites".*Biomacromolecules*, vol. 6, pp.1021-1026

Karthikeyan, V., Dhanapandian, S. and Manoharan, C. (2016). "Characterization and Antibacterial Behavior of MgO Nanoparticles Synthesized via Co-precipitation Method". *International Journal for Scientific Research and Development*, vol. 10(1), pp. 2321-2323

Laranjeiraa, M. S., Moc, A., Ferreira, J., Coimbra, S., Costa, E., Santos-Silva, A., Ferreira, P. J. and Monteiro, F. J. (2016). "Different Hydroxyapatite Magnetic Nanoparticles for Medical Imaging: Its Effects on Hemostatic, Hemolytic Activity and Cellular Cytotoxicity". *Colloids and Surfaces B: Biointerfaces*, vol.146, 363–374

Meyer, B. N., Ferrigni, N. R., Putnam, J. E., Jacobsen, L. B., Nichols, D. E., and McLaughlin, J. L. (1982). "Brine Shrimp: A Convenient General Bioassay for Active Plant Constituents". *Planta Medica*., vol. 45, pp. 31-34

Mishra, U. (2013). *Development of Cobalt-Magnesium Doped Hydroxyapatite for Bone Tissue Engineering Application.* Rourkela: A Project Report Submitted to National Institute of Technology, Department of Biotechnology and Medical Engineering National Institute of Technology, Rourkela

Nakamoto, K. (1970). *Infrared Spectra of Inorganic and Coordination Compounds*. New York: 2nd Edition, Wiley Interscience Publication, pp. 233-235

Rajkumar, M., Sundaram, N. M. and Rajendran, V. (2010). "In-situ Preparation of Hydroxyapatite Nanorod Embedded Poly (Vinyl Alcohol) Composite and its Characterization". *International Journal of Engineering Science and Technology*, vol. 2(6), pp. 2437-2444

Sahgal, G., Ramanathan, S., Sasidlharan, S., Mordi, M. S., Ismail, S. and Mansor, S. M. (2010). "Brine Shrimp Lethality and Acute Oral Toxicity Studies on *Swietenia mahagoni* (Linn.) Jacq. Seed Methanolic Extract". *Pharmacognosy Research*, vol. 2, pp. 215-220

Tawaha, K. A. (2006). "Cytotoxicity Evaluation of Jordanian Wild Plants using Brine Shrimp Lethality Test". *J Appl Sci*., vol. 8(1), pp. 12-17

Wang, H., Li, Y., Zuo, Y., Li, J., Ma, S. and Cheng, L. (2007). "Biocompatibility and Osteogenesis of Biomimetic Nanohydroxyapatite/Polyamide Composite Scaffolds for Bone Tissue Engineering". *Biomaterials*, vol. 28, pp. 3338-3348

Ye, W. and Wang, X. X. (2007). "Ribbon-Like and Rod-Like Hydroxyapatite Crystals Deposited on Titanium Surface with Electrochemical Method". *Mater. Lett*., vol. 61, pp. 4062-4065